Solid State Communications, Vol. 72, No. 5, pp. 507–511, 1989.
Printed in Great Britain.

0038–1098/89 $3.00 + .00
Pergamon Press plc

HIGH-PRESSURE CRYSTAL CHEMISTRY AND AMORPHIZATION OF α-QUARTZ

R.M. Hazen, L.W. Finger, R.J. Hemley and H.K. Mao

Geophysical Laboratory, Carnegie Institution of Washington, 2801 Upton Street NW, Washington, DC 20008-3898, USA

(*Received* 11 *July* 1989 *by G. Burns*)

Single-crystal X-ray diffraction experiments on α-quartz at pressures to 15 GPa reveal structural instabilities that result in its gradual transition to an amorphous state. With increasing pressure the average Si–O distance ($\sim 1.61 \pm 0.01$ Å) and SiO_4 tetrahedral volume ($\sim 2.14 \pm 0.02$ Å^3) remain constant. Compression of α-quartz results from a dramatic decrease in Si–O–Si angle and corresponding decrease in inter-tetrahedral (i.e., O–O) distances. The onset of amorphization coincides with bending of all Si–O–Si angles to less than 120° and severe distortion of SiO_4 tetrahedra, as oxygens approach a close-packed configuration.

α-QUARTZ, the stable 23°C form of SiO_2 between ambient pressure and 3 GPa, persists metastably at room temperature to higher hydrostatic pressures. Above 15 GPa, however, quartz undergoes a gradual transition to an amorphous form [1]. Similar crystalline-to-amorphous transformations induced by high static pressure have been observed in other compounds well below glass-transition temperatures [2–5]. These room-temperature reconstructive transitions are a response to profound structural strain with changing pressure. The transition observed in $LiKSO_4$, for example, has been attributed [4] to extreme distortion of tetrahedral 6-rings, which are unable to conform to size constraints of very compressible potassium–oxygen bonds. Previous studies indicate the transition in quartz may be associated with mechanical instabilities of the structure at high compression [1], but the structure of the material near the onset of the transition has not yet been determined; hence, the structural basis of these instabilities is not known. Crystal-structure refinements on quartz at high pressure [6–8] revealed systematic variations in interatomic distances and angles, but these investigations were limited to pressures of a few GPa, well below the crystalline-to-amorphous transition. In this report we identify a gradual shift of quartz anions to a close-packed arrangement, leading to unstable Si–O–Si and O–Si–O angles, based on single-crystal, X-ray diffraction studies to pressures above 15 GPa.

We selected a 30 × 30 × 10 μm crystal fragment of pure synthetic quartz for high-pressure study. This usually small crystal size is necessary to prevent crystal crushing in diamond-anvil cell experiments above 10 GPa. Room-pressure unit-cell and structure data, obtained on a Rigaku AFC-5 diffractometer with rotating anode generator (graphite-monochromatized Mo$K\alpha$ radiation), agree with previously published results on quartz at ambient conditions [8]. Most quartz crystals display Dauphiné twinning, for which the twin law is a 60° rotation about the trigonal c axis [9]. Our room-pressure structure refinement included a fractional Dauphiné twin parameter, which converged to 0.035 ± 0.003; thus, 96.5% of the fragment is in one orientation, while 3.5% has the other.

We mounted the quartz fragment in a diamond-anvil pressure cell modified for single-crystal X-ray diffraction studies [10, 11]. Neon gas, loaded at high pressure, was employed as the pressure medium. An automated Huber four-circle diffractometer with graphite-monochromatized Mo$K\alpha$ radiation provided diffraction data. We used the eight-reflection centering procedure of King and Finger [12] to measured unit-cell parameters at seven pressures to 15.3 GPa, as recorded in Table 1. Pressure–volume data fit to a Birch–Murnaghan equation of state yield a bulk modulus, K_0, of 34 ± 4 GPa and pressure derivative K_0' of 5.7 ± 0.9. These values are consistent with the lower pressure static compression measurements by Levien *et al.* [8], who obtained 37.1 ± 0.2 GPa and 6.2 ± 0.1, respectively.

α-Quartz compression is anisotropic with the a axis approximately 60% more compressible than c at room pressure. The c/a axial ratio thus increases with pressure. Pressure–length data for both axes can be represented by second-order polynomial equations:

$$a = 4.890(4) - 0.041(2)P + 0.0010(1)P^2,$$

$$c = 5.380(9) - 0.029(3)P + 0.0010(2)P^2,$$

where P is pressure in GPa. Large P^2 terms for both axes indicate significant curvature, which is related to the unusually high K_0'.

The crystal's small size, coupled with the intrinsically weak X-ray scattering efficiency of quartz, result in low peak-to-background ratios. Standard high-pressure data collection of all the several hundred accessible reflections fails to yield enough observations for successful refinement. Instead we employed a revised procedure [13] whereby a subset of only about 100 reflections – those most influenced by variable atom positional parameters – are scanned slowly (approximately 30 min per reflection) to improve peak-to-background. By counting this subset of reflections for relatively long times we increase the number of observed reflections and decrease the estimated standard deviations of those observations. α-Quartz (hexagonal, space group $P3_121$) has four variable atom coordinates: the x silicon and x, y and z oxygen. We refined only those four positional parameters, a scale factor, and an isotropic extinction parameter [14]; the twin fraction and thermal parameters, which are not expected to change significantly with pressure [6], were constrained to their room-pressure values.

Intensity data collected at 2.0, 5.0, 8.0 and 9.5 GPa exhibit sharp diffraction maxima, but at 12.5 GPa, well within the hydrostatic range of the neon pressure medium, slight peak broadening and a corresponding decrease in peak-to-background ratio occurred. This broadening worsened at 15.3 GPa so that the already weak peaks were difficult to center and data collection yielded too few observed reflections for meaningful refinement. Upon release of pressure the peaks remained broad, though the crystal was neither crushed nor otherwise obviously mechanically damaged. We interpret this irreversible crystal degradation in a quasi hydrostatic medium as evidence for the onset of amorphization. In contrast, the weakening and broadening of peaks in both the Raman and powder energy dispersive X-ray diffraction spectra, do not occur until somewhat higher pressures are reached (above ~ 20 GPa) [1]. The present single-crystal X-ray diffraction data therefore provide a more sensitive measurement of the onset of pressure-induced amorphization, because X-ray peak shape is extremely sensitive to changes in mosaic spread (i.e., long-range order).

Conditions of refinement and refined parameters are recorded in Table 1, while selected interatomic distances and angles appear in Table 2 with tetrahedral volumes and distortion parameters. Most oxide crystals compress by two principal structural mechanisms: shortening of metal–oxygen distances and reduction of metal–oxygen–metal angles [15]. Only the second of these mechanisms is important in quartz. Within each tetrahedron (Table 2) there is no significant change in Si–O distance; up to 12.5 GPa the average distance remains ~ 1.61 Å, and polyhedral volume is constant at ~ 2.14 Å^3. The apparent slight decrease in Si–O distance reported by Levien *et al.* [8] does not appear to represent statistically significant bond compression.

Virtually all quartz compression results from decrease in inter-polyhedral distances and angles. The

Table 1. Unit-cell parameters, conditions of refinement, and refined parameters, for quartz at several pressures

Parameter	1 bar*	2.0 GPa	5.1 GPa	8.0 GPa	9.5 GPa	12.5 GPa	15.3 GPa
a (Å)	4.914(1)	4.812(1)	4.705(2)	4.625(1)	4.594(2)	4.535(3)	4.47(1)
c (Å)	5.406(1)	5.327(2)	5.250(2)	5.216(2)	5.200(2)	5.170(5)	5.15(1)
V (Å^3)	113.06(4)	106.84(4)	100.65(8)	96.64(6)	95.02(8)	92.09(14)	89.1(7)
No. data	332	37	35	34	34	18	†
Weighted R	3.9	3.3	3.9	3.8	2.6	4.1	
R	3.8	5.4	7.9	6.0	5.5	8.8	
Extinction ($\times 10^4$)	2.4(2)	4.4(7)	3.5(7)	2.7(8)	4.1(7)	7(2)	
x(Si)**	0.4699(2)	0.4646(9)	0.4532(1)	0.4488(12)	0.4492(10)	0.4487(30)	
x(O)	0.4130(5)	0.4093(15)	0.3930(19)	0.3978(20)	0.3864(15)	0.3670(41)	
y(O)	0.2668(5)	0.2778(17)	0.2881(23)	0.3052(21)	0.2952(15)	0.2952(44)	
z(O)	0.2140(3)	0.2264(14)	0.2340(18)	0.2406(18)	0.2406(13)	0.2427(34)	

* All refinements were constrained to have the twin fraction of 0.035(3) and the isotropic temperature factors of 0.51(2) for Si and 0.86(4) for O obtained from the room pressure refinement, which was measured with the crystal in air.

† No intensity data collected at 15.3 GPa due to reflection broadening.

** Silicon position at (x, 0, 1/3) to conform to standard axes and origin for space group. Note that a transformation of $1/3 - z \rightarrow z$ is needed to compare with the usual, incorrect [21] coordinates.

Table 2. Selected interatomic distances (Å) and angles (°), polyhedral volumes, and distortion indices

Parameter	1 bar	2.0 GPa	5.1 GPa	8.0 GPa	9.5 GPa	12.5 GPa
Intratetrahedral distances and angles						
Si–O [2]	1.607(2)	1.593(8)	1.604(10)	1.602(9)	1.596(7)	1.627(21)
Si–O [2]	1.613(2)	1.615(7)	1.623(9)	1.617(10)	1.621(7)	1.628(19)
mean Si–O	1.610	1.604	1.614	1.609	1.608	1.627
O–O [2]	2.648(3)	2.641(8)	2.711(11)	2.689(11)	2.719(8)	2.810(27)
O–O [2]	2.618(2)	2.601(5)	2.607(7)	2.572(7)	2.585(5)	2.618(15)
O–O	2.628(4)	2.649(16)	2.602(19)	2.629(17)	2.605(14)	2.572(37)
O–O	2.613(4)	2.581(13)	2.569(18)	2.617(19)	2.539(12)	2.501(35)
O–Si–O [2]	110.7(1)	110.8(5)	114.3(5)	113.3(5)	115.4(4)	119.4(11)
O–Si–O [2]	108.8(1)	108.4(2)	107.7(3)	106.1(3)	107.0(2)	107.0(7)
O–Si–O	109.1(2)	110.2(6)	106.6(8)	109.6(7)	107.0(6)	104.4(15)
O–Si–O	108.8(2)	108.2(5)	106.4(7)	108.8(7)	105.4(5)	100.5(12)
Intertetrahedral distances and angles						
Si–Si [4]	3.0594(5)	3.005(1)	2.957(2)	2.922(2)	2.906(2)	2.876(3)
O–O [2]	3.414(3)	3.243(10)	3.099(12)	2.953(11)	2.977(9)	2.934(22)
O–O	3.335(4)	3.114(15)	2.921(19)	2.806(18)	2.794(14)	2.719(35)
Si–O–Si	143.6(2)	139.0(5)	132.8(6)	130.4(6)	129.2(4)	124.2(13)
Tetrahedral volume (Å^3) and distortion						
Volume	2.138(4)	2.12(2)	2.14(2)	2.13(2)	2.12(1)	2.16(4)
Quadratic Elongation	1.000(1)	1.001(5)	1.003(6)	1.003(6)	1.006(4)	1.017(11)
Angle Variance	1.1	1.9	14	11	21	63

most striking change occurs to the Si–O–Si bridging angle. This angle decrease, noted in previous studies of quartz to 6 GPa [6, 7, 8], continues to above 12 GPa (Fig. 1). At room pressure the angle is about 144°, similar to the 139° "strain free" Si–O–Si value cited by Liebau [17]. The angle decreases at 12.5 GPa to 124°, less than any previously recorded average Si–O–Si angle [17]. Extrapolation of pressure versus angle data yields an even smaller value of approximately 120° at 15 GPa. Molecular orbital calculations of strain energy versus Si–O–Si angle reveal a sharp increase in strain energy below 120° [18]. Those calculations, coupled with the absence of observed angles less than 120°, suggest that quartz approaches an energetically unfavourable configuration at 15 GPa.

Inter-tetrahedral O–O compression is directly related to bending of Si–O–Si angles. The shortest of these O–O distances at room pressure is about 3.34 Å, a value significantly larger than the 2.63 Å average of intra-tetrahedral O–O distances (Table 2). At 12.5 GPa, however, the shortest inter-tetrahedral distance is only 2.72 Å, well within the range of intra-tetrahedral distances. Furthermore, extrapolation of the structure to higher pressures (Fig. 2) reveals that all oxygens approach a close-packed configuration. Compression of quartz occurs by decreasing the volume between volumetrically rigid tetrahedral units, a process equivalent to increasing the anion packing efficiency. By 15 GPa a quartz achieves a nearly close-packed anion distribution; the *c*-axis channels, characteristic of quartz at room conditions, are virtually closed.

Oxygen close-packing of high-pressure quartz is not ideal. The tetrahedra become highly distorted,

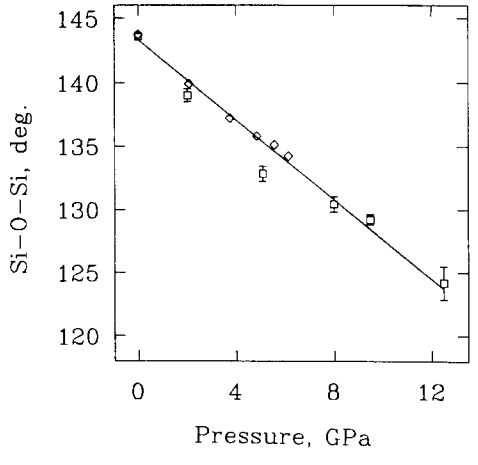

Fig. 1. Si–O–Si angle versus pressure. Square symbols, present results; diamonds, data of Levien *et al.* [8].

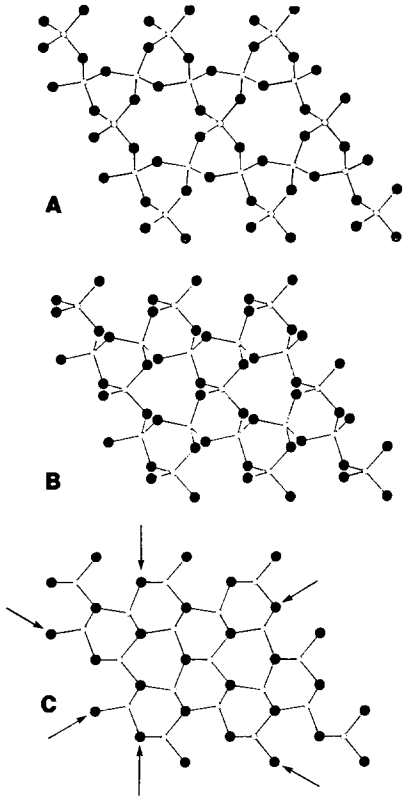

Fig. 2. Projections down the c axis for quartz at (A) room pressure, (B) 12.5 GPa, and (C) extrapolated to maximum Si–O–Si bending. Larger solid circles represent oxygen, whereas smaller open circles denote silicon. With increasing pressure the oxygen atoms approach a close-packed configuration in which the Si–O–Si angle is close to 120° and the tetrahedra are significantly flattened perpendicular to c from their ideal form. Larger 6-tetrahedra helices and smaller 3-tetrahedra helices are distinct in A and B. In C, however, oxygens at (1/3, 1/3, 1/4) superimpose in the (0 0 1) projection, and the diameter of 3- and 6-helices are similar. Arrows indicate planes, oblique to the illustration, of close-packed oxygens. Note, however, that in spite of the regular oxygen spacing in the figure, (0 0 1) is not a close-packed plane because the oxygens are at different z coordinates.

perhaps owing to Si–Si interactions. Levien *et al.* [8] identified a dramatic increase in tetrahedral distortion at pressures to 6 GPa; we observe additional distortion at higher pressures. The silicon tetrahedron is close to ideal at room pressure: two distinct intra-tetrahedral Si–O bond distances differ by less than 0.01 Å, and O–Si–O intra-tetrahedral angles deviate by only about 1° from the ideal 109.5° value. With increasing pressure, however, the Si–O bonds differ by more than 0.02 Å, and angles deviate by several degrees from 109.5. Polyhedral distortion indices – quadratic elongation and angle variance ([16], see Table 2) – reflect these variations. Pressure-induced changes in polyhedral distortions are usually insignificant in oxides and silicates [15]. In quartz, however, as the anion distribution becomes more regular, the quartz tetrahedral distortion exceeds that documented for any other silicate. Extrapolated to its most distorted form (Fig. 2c), the quartz tetrahedron has one O–Si–O angle close to 90° and another close to 130°. The latter angle is sufficiently wide to create a low-energy diffusion channel ("path of escape") for the silicon ion.

Spectroscopic measurements and available equation-of-state data indicate that amorphous forms of SiO_2 with 4-coordinated silicon can achieve a much higher density than quartz [1]. We propose that the high-pressure transition to an amorphous state is driven by the significant volume reduction, and by the alleviation of internal strain due to small Si–O–Si angles and very distorted tetrahedra. One possible mechanism of amorphization and densification might be breaking of highly strained Si–O bonds associated with 130° O–Si–O angles around the perimeter of the larger c-axis channels (Fig. 2), and subsequent relinking across channels. The resultant interpenetrating 6-rings, similar to those observed in the cuprite (Cu_2O) structure, represent a significantly denser packing of tetrahedra, with few broken Si–O bonds. Such a cross-linking mechanism is also consistent with the shear mode instability noted previously [1], based on extrapolation of high-pressure ultrasonic measurements [19]. The present structural results suggest that this instability occurs when SiO_4 tetrahedra are compacted to the maximum degree permitted by the topology of the quartz structure.

Metal–oxygen bond compression and metal–oxygen–metal bending, which are the two principal compression mechanisms in oxides and silicates, may gradually transform a stable structure into one that is topologically untenable. In many framework compounds such instabilities lead to soft-mode, reversible "polyhedral tilt" transitions [20] in which metal–oxygen–metal angles change discontinuously. In some instances, however, polyhedral tilting is not possible. In $CaSiO_3$ perovskite decompression, for example, Si–O–Si angles are already fully stretched to 180°. In quartz compression, on the other hand, Si–O–Si angles are fully bent to 120° at the onset of the glass transition, and oxygens approach the minimum-volume close-packed configuration. It appears, therefore, that localized Si–O bond breaking and consequent pressure-induced amorphization results from bending Si–O–Si groups beyond their energetic limits.

Acknowledgements – We thank Q.C. Williams, C.T. Prewitt, and A.P. Jephcoat for critical reviews of the manuscript. The work was supported in part by National Science Foundation (grants EAR 86-18649 and EAR 87-08192) and by the Carnegie Institution of Washington.

REFERENCES

1. R.J. Hemley, in *High-Pressure Research in Mineral Physics* (Edited by M.H. Manghnani & Y. Syono), p. 347, Terra Scientific, Tokyo/ Americal Geophysical Union, Washington, D.C., (1987); R.J. Hemley, A.P. Jephcoat, H.K. Mao, L.C. Ming & M.H. Manghnani, *Nature* **334,** 52 (1988).
2. O. Mishima, L.D. Calvert & E. Whalley, *Nature* **310,** 393 (1984).
3. Y. Fujii, M. Kowaka & A. Onodera, *J. Phys. C. Solid State Phys.* **18,** 789 (1985).
4. H. Sankaran, S.K. Sikka, S.M. Sharma & R. Chidambaram, *Phys. Rev. B* **38,** 170 (1988).
5. Q. Williams & R. Jeanloz, *Nature,* **338,** 413 (1989).
6. J.D. Jorgenson, *J. Appl. Phys.* **49,** 5473 (1978).
7. H. d'Amour, W. Denner & H. Schultz, *Acta Crystallogr.* **B35,** 550 (1979).
8. L. Levien, C.T. Prewitt & D.J. Weidner, *Am. Mineral.* **65,** 920 (1980).
9. W.A. Deer, R.A. Howie & J. Zussman, *Rock-Forming Minerals* New York: Wiley (1966).
10. H.K. Mao & P.M. Bell, *Carnegie Inst. Wash. Year Book* **79,** 409 (1980).
11. R.M. Hazen & L.W. Finger, *Comparative Crystal Chemistry* New York: Wiley (1979).
12. H.E. King & L.W. Finger, *J. Appl. Cryst.* **12,** 374 (1979).
13. R.M. Hazen & L.W. Finger, *Am. Mineral.* **74,** 352 (1989).
14. P.J. Becker & P. Coppens, *Acta Crystallogr.* **A30,** 129 (1974).
15. R.M. Hazen & L.W. Finger, *Science. Am.* **252,** 110 (1985).
16. K. Robinson, G.V. Gibbs & P.H. Ribbe, *Science* **172,** 567 (1971).
17. F. Liebau, *Structural Chemistry of Silicates.* New York: Springer (1985). The smallest individual Si–O–Si angle with 2-coordinated bridging oxygen in room-pressure silicates is about 135°, and the average Si–O–Si angle in framework silicates is close to 140° (6). A single Si–O–Si angle of 132° was reported in the coesite form of SiO_2 at 5.2 GPa (L. Levien & C.T. Prewitt, *Amer. Miner.* **66,** 324 1981), but the other bridging angles range up to 180°, yielding an average Si–O–Si greater than 140° for that high-pressure structure.
18. K.L. Geisinger, G.V. Gibbs & A. Navrotsky, *Phys. Chem. Minerals* **11,** 266 (1985).
19. H.J.P. McSkimin, P. Andreatch & R.N. Thurston, *J. Appl. Phys.* **36,** 1624 (1965).
20. R.M. Hazen & L.W. Finger, *Phase Transitions* **1,** 1 (1979).
21. T.H.K. Barron, C.C. Huang & A. Pasternak, *J. Phys. C: Solid State Phys.* **9,** 3925 (1976).